

## SPECTRUM OF COHERENT BACKSCATTERING OF LIGHT BY TWO ATOMS

© 2007 г. V. N. Shatokhin

*B.I. Stepanov Institute of Physics, National Academy of Sciences, 220072 Minsk, Belarus*

*e-mail: v.shatokhin@dragon.bas-net.by*

Received October 12, 2006

**Abstract**—We study theoretically inelastic spectrum of coherent backscattering of laser light by two atoms was theoretically studied. For an intense laser field, there are frequency domains of either constructive or destructive self-interference of inelastically scattered photons. The emergent spectral features by considering coherent backscattering was interpreted as a pump-probe experiment.

PACS: 42.50.Ct, 42.25.Dd, 32.80.-t, 42.25.Hz

### 1. INTRODUCTION

Coherent backscattering (CBS) of resonant laser light – an interferential enhancement of the average intensity of light reflected off a dilute, disordered medium in the backscattering direction – has recently been observed with cold, trapped atomic clouds [1, 2]. It was immediately recognized that such an experimentally very well controlled quantum system as an atomic medium bears a great potential for studying localization and transport phenomena in mesoscopic systems, which was hitherto possible only with classical particles scattering photons, or with disordered solids scattering electrons [3]. Since then, CBS of light by cold atoms has become an area of intense theoretical and experimental research (for a recent review, see [4]).

The underlying physical reason for the emergence of CBS is constructive interference between the counterpropagating (labelled “direct” and “reversed”) multiple scattering amplitudes. When a scattering medium consists of individual atoms, several mechanisms affecting phase coherence between the interfering waves should be considered. These are (i) Raman scattering on degenerate atomic transitions; (ii) inelastic scattering; (iii) mechanical motion of atoms.

As regards the atomic degeneracy mediating Raman processes accompanied by photon polarization flips, its dephasing role is nowadays very well understood, with quantitative accordance between theory [5–7] and experiment [2, 8], for ensembles of Rb atoms.

The next dephasing mechanism, the inelastic photon scattering induced by atomic saturation  $s$ , has been studied in less detail. Recent experiment with cold Sr atoms [9] demonstrated a rapid decrease of CBS enhancement factor  $\alpha$  versus saturation at moderate  $s \leq 1$ . It was shown, within a scattering theory approach applied to two atoms in the regime of weakly nonlinear scattering [10], that a decrease of CBS enhancement factor occurs due to the partial distinguishability of the

interfering amplitudes. In the general case of many atoms, three different amplitudes interfere constructively in the weakly nonlinear regime, so that  $\alpha$  may exceed the linear barrier 2 [11].

In this contribution, we will also be concerned with the impact of saturation on CBS, though for arbitrary laser field intensities. But prior to proceed with a presentation of this work, let us make a brief note on the effect of thermal motion of atoms at temperatures on the order 100  $\mu$ K typical for CBS experiments.

Mechanical motion spoils phase coherence between the direct and reversed amplitudes [12], if spread  $v$  of the atomic velocities violates the resonance condition  $k v \ll 2\gamma$  [13], where  $k$  is the wave number and  $2\gamma$  is the natural linewidth of the excited atomic state. In the regime of weak laser intensities, the inequality is usually satisfied, and the picture of motionless atoms works very well so long as the CBS intensity is concerned [5]. However, already in the elastic scattering regime, the photon recoil and Doppler effects do modify the CBS spectrum [14]. It is even more so in the inelastic scattering regime, when the atoms from the cloud are rapidly accelerated out of resonance by a powerful laser field. Nonetheless, we will ignore this acceleration, and assume that the atoms are fixed in space. Thus, we focus here on the laser field coupling exclusively to the atomic internal degrees of freedom, in order to highlight the fundamental interference effect under the influence of nonlinear scattering. Explanation of this influence for atoms at rest is basic to its understanding for atoms in motion.

More specifically, we will study spectrum of CBS by two atoms in the helicity preserving channel, for arbitrary intensities of the laser field. This topic is above all motivated by our previous work [15, 16], where we established existence of the residual CBS contrast in the deep saturation regime, due to the constructive self-interference of inelastically scattered photons. However,

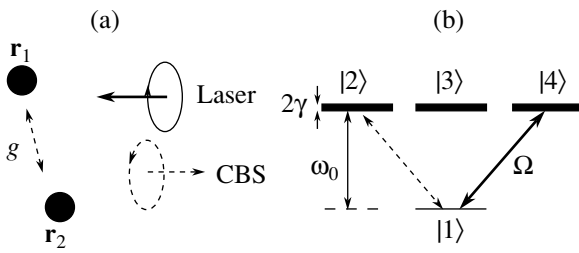


**Fig. 1.** Model of CBS with two atoms. (a) atoms (black dots) are driven by laser light with right circular polarization, while CBS is observed in the helicity preserving channel, that is, with flipped polarization. Photons in this channel appear as a result of double scattering.  $g$  is the strength of the far-field dipole-dipole coupling responsible for exchange of photons; (b) internal atomic structure corresponding to a  $J_g = 0 \rightarrow J_e = 1$  dipole transition.  $\omega_0$  is the transition frequency,  $2\gamma$  is the radiative linewidth,  $\Omega$  is the Rabi frequency. Sublevels  $|1\rangle$  and  $|3\rangle$  have magnetic quantum number  $m = 0$ . Sublevels  $|2\rangle$  and  $|4\rangle$  correspond to  $m = -1$  and  $m = 1$ , respectively. Thick solid arrow shows laser field driving  $|1\rangle \leftrightarrow |4\rangle$  transition, while dashed arrow shows CBS field originating from  $|1\rangle \leftrightarrow |2\rangle$  transition.

this constructive interference is a net effect of all inelastic photons. The question that naturally arises, of what the character of interference is at a given frequency, can only be answered after looking at the CBS spectrum. In this work we find CBS spectrum and answer this question for the particular case of exact resonance. We demonstrate that, in the deep saturation regime, there are frequency domains in the CBS spectrum exhibiting either constructive or destructive interference, and employ the dressed states representation to identify the scattering processes that are responsible for the emergent spectral features. Our results agree with those derived within the Langevin equation approach [17].

The paper is organized as follows: We start with a brief presentation of our model and the master equation approach that we are using. In Sect. 3 we present results for the stationary CBS intensity and enhancement factor, and thereafter for CBS spectrum. In the last Section, we conclude our work.

## 2. MASTER EQUATION APPROACH TO CBS OF LIGHT BY TWO ATOMS

### A. Model and the Main Quantity of Interest

Details of our approach are given in Ref. [16]. Here, we will only present its brief outline. We consider a model quantum system consisting of 2 identical motionless atoms located at positions  $\mathbf{r}_1$  and  $\mathbf{r}_2$ , with the distance  $r_{12} = |\mathbf{r}_1 - \mathbf{r}_2|$  being much greater than the optical wavelength. The atoms are embedded in the electromagnetic bath of quantized harmonic oscillators and subjected to an external laser field of arbitrary intensity (see Fig. 1a). Coupling to the bath gives rise to the spontaneous emission from the excited state and to the far-field dipole-dipole interaction responsible for ex-

change of photons, whereas coupling to the laser field gives rise to the Rabi oscillations of populations and coherences in the laser-driven transitions of both atoms. Although the approach can, of course, be formulated for atoms with arbitrary internal structure, we choose the ground states of the atoms to be nondegenerate, while the excited state 3-fold degenerate (see Fig. 1b). An important parameter describing the effect of a laser field on atoms is the so-called saturation parameter  $s = \Omega^2/2(\gamma^2 + \delta^2)$ , where  $\Omega$  is the Rabi frequency, and  $\delta = \omega_L - \omega_0$  is the detuning of the laser field with respect to atomic resonance. As already mentioned, we will be interested in how spectrum of CBS depends on  $s$  (or  $\Omega$ ).

Raman processes which can strongly affect CBS do not take place on the  $J_g = 0 \rightarrow J_e = 1$  transition under consideration. Furthermore, incoherent single scattering contribution can be filtered out, by looking at CBS, e.g., in the helicity preserving ( $h \parallel h$ ) polarization channel. Precisely this channel was probed in a recent experiment with cold Sr atoms [9]. We consider the particular case of the laser light with the right circular polarization, that is,  $\boldsymbol{\epsilon}_L = \hat{\mathbf{e}}_{+1}$ , in the helicity basis notation. Hence, CBS with preserved helicity corresponds to the flipped polarization  $\boldsymbol{\epsilon} = \hat{\mathbf{e}}_{-1}$  as shown on Fig. 1.

Spectrum of CBS to be addressed in this paper is derived from the average value of the first-order field temporal correlation function [18]:

$$G^{(1)}(\mathbf{r}, t; \mathbf{r}, t') = \langle \text{Tr} \{ \rho [ \boldsymbol{\epsilon} \mathbf{E}^{(-)}(\mathbf{r}, t) ] [ \boldsymbol{\epsilon}^* \mathbf{E}^{(+)}(\mathbf{r}, t') ] \} \rangle_{\text{conf}}, \quad (1)$$

where  $\rho$  is the initial density operator of the atom-field system,  $\mathbf{E}^{(-/+)}(\mathbf{r}, t)$  is the negative/positive frequency component of the electric field operator of the scattered field, and  $\langle \dots \rangle_{\text{conf}}$  denotes configuration averaging. The components of the scattered field are the retarded fields radiated by the atomic dipoles,

$$\mathbf{E}^{(+)}(\mathbf{r}, t) = \frac{\omega_0^2}{4\pi\epsilon_0 c^2 r} \sum_{\alpha=1}^2 \mathbf{D}_{\alpha}(t_{\alpha}) e^{-i\mathbf{k}\mathbf{r}_{\alpha}}, \quad (2)$$

where  $\epsilon_0$  is the permittivity of the vacuum,  $\mathbf{D}_{\alpha} = -\hat{\mathbf{e}}_{-1} \sigma_{12}^{\alpha} + \hat{\mathbf{e}}_0 \sigma_{13}^{\alpha} - \hat{\mathbf{e}}_{+1} \sigma_{14}^{\alpha}$ , with  $\sigma_{kl}^{\alpha} \equiv |k\rangle_{\alpha} \langle l|_{\alpha}$ , is the dipole lowering operator, and  $t_{\alpha} = t - |\mathbf{r} - \mathbf{r}_{\alpha}|/c$ . In writing Eq. (2), we have assumed that  $r_{12} \ll r$ , that is, the field is detected in the radiation zone at the distance much larger than the interatomic distance. In the following, we will for brevity omit the  $r$ -dependent prefactor of Eq. (2) and, consistently, of the temporal correlation functions.

Inserting Eq. (2) into Eq. (1) we obtain, in the steady state limit  $t \rightarrow \infty$ ,

$$G_{ss}^{(1)}(\tau) = \sum_{\alpha, \beta=1}^2 \langle \langle \sigma_{21}^\alpha \sigma_{12}^\beta(\tau) \rangle \rangle_{ss} e^{ik\mathbf{r}_{\alpha\beta}} \rangle_{\text{conf}}, \quad (3)$$

where “ss” stands for *steady state*,  $\tau = t' - t \geq 0$ , the inner angular brackets indicate quantum mechanical expectation value [see Eq. (1)], and  $\mathbf{r}_{\alpha\beta} \equiv \mathbf{r}_\alpha - \mathbf{r}_\beta$ .

Spectrum can be obtained via Laplace transform of (3) [19]:

$$S(\nu) = \frac{1}{\pi} \lim_{\Gamma \rightarrow 0} \text{Re} \{ \tilde{G}_{ss}^{(1)}(z) \}, \quad (4)$$

where  $\tilde{G}_{ss}^{(1)}(z) = \int_0^\infty d\tau \exp(-z\tau) G_{ss}^{(1)}(\tau)$ ,  $z = \Gamma - i\nu$  with  $\Gamma \geq 0$  and  $\nu = \omega - \omega_L$ . Note that the spectrum is defined with respect to the laser frequency which means that the atomic correlation functions must be evaluated in the frame rotating at  $\omega_L$ .

Let us conclude this subsection with a remark on the configuration averaging procedure. This procedure is necessary because the two-atom correlation functions may sensitively depend on the interatomic distance and orientation of the vector  $\mathbf{r}_{12}$  with respect to  $\mathbf{k}_L$ , exhibiting rapid oscillations around the backscattering direction. These oscillations have the same nature as a speckle pattern scattered off a disordered medium. After many realizations of the disorder, all peaks except the one, corresponding to CBS, disappear. A simple and sufficient way to mimic disorder in a two-atom system is to assume an isotropic distribution of the radius-vector connecting the atoms and a uniform distribution of interatomic distances around the average distance  $l$  equal to the scattering mean free path.

### B. Master Equation

To find the atomic correlation functions appearing in the right hand side of Eq. (3) we have adapted [15, 16] a theoretical approach initiated by Lehmborg in 1970 [20]. Within this approach, dynamics of the dipole operators' expectation values as well as dipole-dipole correlators is governed by the master equation

$$\langle \dot{Q} \rangle = \sum_{\alpha=1}^2 \langle \mathcal{L}_\alpha Q \rangle + \sum_{\alpha \neq \beta=1}^2 \langle \mathcal{L}_{\alpha\beta} Q \rangle, \quad (5)$$

where the Liouvillians  $\mathcal{L}_\alpha$  and  $\mathcal{L}_{\alpha\beta}$  generate the time evolution of an arbitrary atomic operator  $Q$ , for independent and interacting atoms, respectively. Explicitly,

$$\begin{aligned} \mathcal{L}_\alpha Q &= -i\delta[\mathbf{D}_\alpha^\dagger \mathbf{D}_\alpha, Q] - \\ &- \frac{i}{2} [\Omega_\alpha (\mathbf{D}_\alpha^\dagger \boldsymbol{\varepsilon}_L) + \Omega_\alpha^* (\mathbf{D}_\alpha \boldsymbol{\varepsilon}_L^*), Q] + \\ &+ \gamma (\mathbf{D}_\alpha^\dagger [Q, \mathbf{D}_\alpha] + [\mathbf{D}_\alpha^\dagger, Q] \mathbf{D}_\alpha), \end{aligned} \quad (6)$$

$$\begin{aligned} \mathcal{L}_{\alpha\beta} Q &= \mathbf{D}_\alpha^\dagger \overset{\leftrightarrow}{\mathbf{T}}(g, \hat{\mathbf{n}}) [Q, \mathbf{D}_\beta] + \\ &+ [\mathbf{D}_\beta^\dagger, Q] \overset{\leftrightarrow}{\mathbf{T}}^*(g, \hat{\mathbf{n}}) \mathbf{D}_\alpha, \end{aligned} \quad (7)$$

where  $\Omega_\alpha = \Omega e^{ik_L r_\alpha}$  is the position-dependent Rabi frequency. The radiative dipole-dipole interaction due to exchange of photons between the atoms is described by the tensor  $\overset{\leftrightarrow}{\mathbf{T}}(g, \hat{\mathbf{n}}) = \gamma g \overset{\leftrightarrow}{\mathbf{\Delta}}$ , with  $\overset{\leftrightarrow}{\mathbf{\Delta}} = \overset{\leftrightarrow}{\mathbf{1}} - \hat{\mathbf{n}}\hat{\mathbf{n}}$  being the projector on the transverse plane defined by the unit vector  $\hat{\mathbf{n}}$  along the connecting line between the atoms  $\alpha$  and  $\beta$ . This interaction has a certain strength depending on the distance between the atoms, via

$$g = \frac{3i}{2k_0 r_{\alpha\beta}} e^{ik_0 r_{\alpha\beta}}, \quad (8)$$

with  $k_0 = \omega_0/c$ , and on the life time of the excited atomic levels, through  $\gamma$ . The coupling constant  $|g| \ll 1$  is small in the far-field ( $k_0 r_{\alpha\beta} \gg 1$ ), where near-field interaction terms of order  $(k_0 r_{\alpha\beta})^{-2}$  and  $(k_0 r_{\alpha\beta})^{-3}$  can be neglected.

Of course, an arbitrary operator  $Q$  inserted into Eq. (5) does not result in a closed differential equation. Our system consisting of two four-level atoms leads to  $255 = 4^2 \times 4^2 - 1$  linear coupled equations of motion for the one-time averages. We solve them perturbatively up to  $g^2$ , to account for the lowest order (double-)scattering process giving rise to a nontrivial interferential contribution. To help the reader keeping this in mind we will supply symbols denoting double scattering intensities and spectra with the subscript “2”.

Note that Eq. (5) describes evolution of the expectation values (one-time correlation functions), whereas  $G_{ss}^{(1)}(\tau)$  is the *two-time* correlation function. By virtue of the quantum regression theorem [19], the latter satisfy Eq. (5) also, but their initial conditions are extracted from the stationary solution of (5). In particular, the double scattering counterpart of  $G_{ss}^{(1)}(0)$  is nothing but the stationary average backscattered light intensity which will be referred to as  $I_2^{\text{tot}}$ . There is an obvious relation between  $I_2^{\text{tot}}$  and  $S_2(\nu)$ :

$$I_2^{\text{tot}} = \int_{-\infty}^{\infty} d\nu S_2(\nu). \quad (9)$$

The expression for  $I_2^{\text{tot}}$  can be obtained independently from (9). We will use this independent derivation as an implicit verification of our results for CBS spectra.

The total CBS intensity at the backscattering direction can be decomposed in the sum of two terms

$$I_2^{\text{tot}} = L_2^{\text{tot}} + C_2^{\text{tot}}, \quad (10)$$

where  $C_2^{\text{tot}} \equiv C_2^{\text{tot}}(\theta = 0)$  (i.e.,  $\mathbf{k} = -\mathbf{k}_L$ ), and

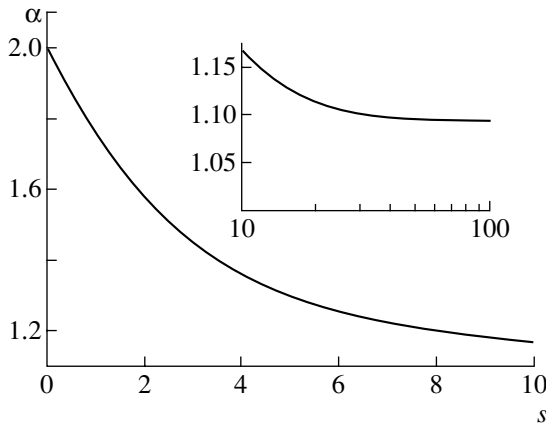


**Fig. 2.** Enhancement factor in the  $h \parallel h$  channel versus saturation  $s$ . Decrease of  $\alpha$  at small  $s$  is described by the linear function  $2 - s/4$  in accordance with [10]. Inset describes  $\alpha$  in the deep saturation regime. Enhancement tends to the limit  $\alpha_\infty = 23/21$  [16] indicating constructive self-interference of inelastic photons.

$$C_2^{\text{tot}}(\theta) = 2 \text{Re} \langle \langle \sigma_{21}^1 \sigma_{12}^2 \rangle_{\text{ss}}^{[2]} e^{i\mathbf{k}\mathbf{r}_{12}} \rangle_{\text{conf}}, \quad (11)$$

$$L_2^{\text{tot}} = \langle \langle \sigma_{22}^1 \rangle_{\text{ss}}^{[2]} + \langle \sigma_{22}^2 \rangle_{\text{ss}}^{[2]} \rangle_{\text{conf}}, \quad (12)$$

are the so called crossed and ladder terms, respectively. Using these terms, we can derive a standard measure of phase coherence between the counterpropagating amplitudes in CBS – the enhancement factor

$$\alpha = 1 + \frac{C_2^{\text{tot}}}{L_2^{\text{tot}}}, \quad (13)$$

which for perfect two-wave interference is equal to 2.

Generally, the total backscattered light intensity has the elastic and inelastic counterparts,

$$I_2^{\text{tot}} = I_2^{\text{el}} + I_2^{\text{inel}}. \quad (14)$$

The elastic counterpart is given by the product of the expectation values of the atomic dipoles,

$$I_2^{\text{el}} = \sum_{\alpha, \beta=1}^2 \langle \langle \sigma_{21}^\alpha \rangle_{\text{ss}} \langle \sigma_{12}^\beta \rangle_{\text{ss}} e^{-i\mathbf{k}_L \mathbf{r}_{\alpha\beta}} \rangle_{\text{conf}}, \quad (15)$$

wherefrom for  $\alpha = \beta$  we obtain the elastic ladder term  $L_2^{\text{el}}$  and for  $\alpha \neq \beta$  the elastic crossed term  $C_2^{\text{el}}$ . Given  $I_2^{\text{tot}}$  and  $I_2^{\text{el}}$  we can find the fluctuating part of the dipole correlation functions defining  $I_2^{\text{inel}}$ .

### 3. RESULTS

We will restrict our consideration to the case of exact resonance,  $\delta = 0$ . An important advantage of this choice is that all results can be deduced analytically.

Numerical results for  $\delta \neq 0$  will be presented in a separate contribution.

#### A. CBS Intensity and Enhancement Factor

The interferential contribution and the incoherent sum, Eqs. (11) and (12), yield results [16]

$$2 \text{Re} \{ \langle \sigma_{21}^1 \sigma_{12}^2 \rangle_{\text{ss}}^{[2]} e^{i\mathbf{k}\mathbf{r}_{12}} \} = |g|^2 |\tilde{\Delta}_{+,+1}^\leftrightarrow|^2 \frac{R_1(s)}{(4+s)P(s)} \cos \{ (\mathbf{k} + \mathbf{k}_L) \mathbf{r}_{12} \}, \quad (16)$$

$$\langle \sigma_{22}^1 \rangle_{\text{ss}}^{[2]} + \langle \sigma_{22}^2 \rangle_{\text{ss}}^{[2]} = |g|^2 |\tilde{\Delta}_{+,+1}^\leftrightarrow|^2 \frac{R_2(s)}{P(s)}. \quad (17)$$

$R_1(s)$ ,  $R_2(s)$ , and  $P(s)$  are polynomial expressions in the on-resonance saturation parameter  $s = \Omega^2/2\gamma^2$ ,

$$R_1(s) = \frac{2}{9}(6912s + 3168s^2 + 264s^3 + 20s^4 + s^5), \quad (18a)$$

$$R_2(s) = \frac{1}{3}(1152s + 528s^2 + 132s^3 + 7s^4), \quad (18b)$$

$$P(s) = (1+s)^2(12+s)(32+20s+s^2), \quad (18c)$$

and  $\tilde{\Delta}_{+,+1}^\leftrightarrow = \hat{\mathbf{e}}_{+1} \tilde{\Delta} \mathbf{e}_{+1}$ .

The configuration average of (16) and (17) leads to the final result

$$C_2^{\text{tot}}(\theta) \approx \frac{|\tilde{g}|^2 R_1(s)}{(4+s)P(s)} \left( \frac{2}{15} - \frac{(k\theta)^2}{35} \right), \quad (19)$$

$$L_2^{\text{tot}} = \frac{2|\tilde{g}|^2 R_2(s)}{15P(s)}, \quad (20)$$

with  $\tilde{g} = g|_{r_{\alpha\beta}=l}$ . The scattering angle  $\theta = 2 \arcsin \{ |\mathbf{k} + \mathbf{k}_L|/2k_L \} \ll 1$  with respect to the backscattering direction was assumed to be sufficiently small herein.

The inhanement factor  $\alpha(s)$ , Eq. (13), deduced from Eqs. (19) and (20) reads

$$\alpha(s) = 1 + \frac{R_1(s)}{(4+s)R_2(s)}, \quad (21)$$

and  $\alpha(0) = 2.0$  in the weak field limit, as expected. The dependence of  $\alpha$  on the saturation parameter is shown on Fig. 2. For small  $s$ , enhancement linearly decreases as  $2 - s/4$ , in full agreement with the diagrammatic theoretical result [10] and in qualitative agreement with the result of Sr experiment [9]. When  $s$  increases further,  $\alpha$  monotonically drops to an asymptotic value  $\lim_{s \rightarrow \infty} \alpha(s) = \alpha_\infty = 23/21$  [16] which is strictly larger than

unity, implying a nonvanishing residual CBS contrast in the limit of large injected intensities. We will next show that this residual enhancement is due to inelastic

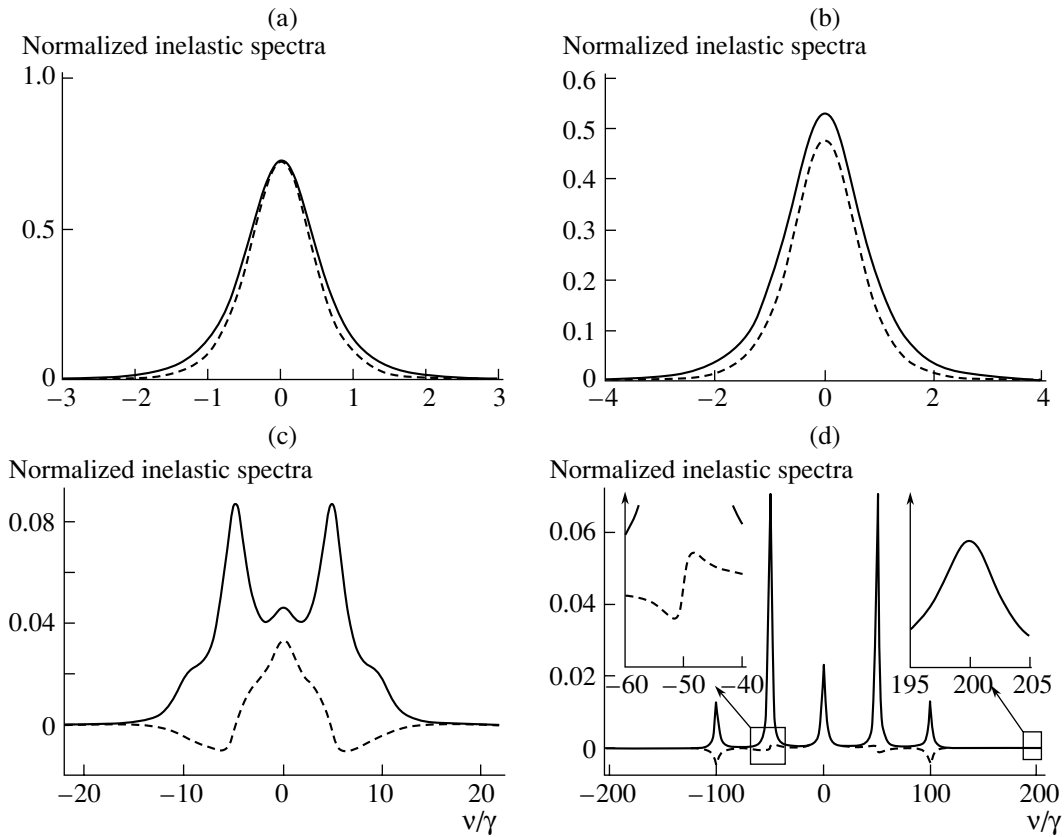


**Fig. 3.** Normalized inelastic spectra of the ladder (solid line) and crossed (dashed line) terms at exact resonance for different values of the Rabi frequency: (a)  $\Omega = 0.1\gamma$ , (b)  $\Omega = \gamma$ , (c)  $\Omega = 10\gamma$ , (d)  $\Omega = 100\gamma$ .

photons only. Indeed, we obtained the following result for the elastic ladder and crossed terms

$$L_2^{\text{el}} = C_2^{\text{el}} = \frac{2|\tilde{g}|^2 s}{15(1+s)^4}. \quad (22)$$

As seen from Eq. (22) the elastic component shows perfect contrast for all  $s$ . In particular, it is this component

that results in enhancement  $\alpha = 2$  for very small  $s \rightarrow 0$ . However, in the deep saturation regime, this component decreases as  $s^{-3}$ , while the counterparts of the total intensity, Eqs. (19), (20), as  $s^{-1}$ . Herefrom follows our conclusion about the origin of the residual enhancement in the deep saturation regime. Explicitly, the inelastic crossed and ladder terms obtained by elementary subtraction of Eq. (22) from Eqs. (19) and (20) read

$$C_2^{\text{inel}} = \frac{2|\tilde{g}|^2 (20736s^2 + 23424s^3 + 7108s^4 + 601s^5 + 44s^6 + 2s^7)}{15 \cdot 9(1+s)^2(4+s)P(s)}, \quad (23)$$

$$L_2^{\text{inel}} = \frac{2|\tilde{g}|^2 (2016s^2 + 2244s^3 + 796s^4 + 146s^5 + 7s^6)}{15 \cdot 3(1+s)^2P(s)}. \quad (24)$$

It is easy to verify that  $\lim_{s \rightarrow \infty} C_2^{\text{inel}}/L_2^{\text{inel}} = 2/21 = \alpha_\infty - 1$ .

### B. CBS Spectrum

Double scattering spectrum of CBS has the elastic and inelastic components. The elastic spectrum at the backscattering direction reads

$$\tilde{I}_2^{\text{el}}(\nu) = I_2^{\text{el}}\delta(\nu), \quad (25)$$

where  $\delta(\nu)$  is the Dirac's delta-function, and  $I_2^{\text{el}} = L_2^{\text{el}} + C_2^{\text{el}}$ , with the ladder and crossed contributions defined in Eq. (22).

Inelastic spectra of the normalized ladder and crossed terms, for increasing values of Rabi frequencies, are shown on Fig. 3. Normalization is chosen such

that integrals of  $\tilde{L}_2^{\text{inel}}(\nu)/L_2^{\text{inel}}$  and  $\tilde{C}_2^{\text{inel}}(\nu)/L_2^{\text{inel}}$  over  $\nu$  yield unity and  $C_2^{\text{inel}}/L_2^{\text{inel}}$ , respectively. In the deep saturation regime, the value of the latter integral tends to the asymptotic value of the interference contrast of CBS,  $\alpha_\infty - 1$ .

In describing the CBS spectrum, it is natural to use two parameters  $\Omega$  and  $\gamma$  defining positions and linewidths of spectral peaks rather than a single saturation parameter  $s$ . We will utilize  $s$  only to check consistency of our expressions for spectra with the results for the inelastic intensity and the enhancement factor.

As seen from Fig. 3, inelastic spectra are symmetric with respect to the laser frequency, for all  $\Omega$ . For a small value of the Rabi frequency  $\Omega = 0.1\gamma$  (Fig. 3a), spectra of both the ladder and crossed contributions have single peaks at  $\nu = 0$ . Interferential contribution  $\tilde{C}_2^{\text{inel}}(\nu)$  is constructive, though  $\tilde{C}_2^{\text{inel}}(\nu) \leq \tilde{L}_2^{\text{inel}}(\nu)$  indicating that interference is not perfect in this weakly inelastic regime. We can derive analytical expressions for the curves of Fig. 3a by leaving the leading order contribution to inelastic scattering  $\sim(\Omega/\gamma)^4$ , corresponding to two-photon processes, and neglecting the higher-order terms.

The ladder and crossed terms yield the compact expressions (henceforth, we will omit the common prefactor  $2|\tilde{g}|^2/15$ ):

$$\begin{aligned} \tilde{L}_2^{\text{inel}}(\nu) &\approx \frac{1}{\pi} \left(\frac{\Omega}{\gamma}\right)^4 \frac{\gamma^3(2\gamma^2 + \nu^2)}{2(\gamma^2 + \nu^2)^3}, \\ \tilde{G}_2^{\text{inel}}(\nu) &\approx \frac{1}{\pi} \left(\frac{\Omega}{\gamma}\right)^4 \frac{\gamma^5}{(\gamma^2 + \nu^2)^3}. \end{aligned} \tag{26}$$

It is easy to establish that the expressions in Eq. (26) are consistent with the behavior of the enhancement factor in the two-photon scattering regime. Integrating  $\tilde{L}_2^{\text{inel}}(\nu)$ ,  $\tilde{C}_2^{\text{inel}}(\nu)$  over all frequencies, we obtain the following inelastic ladder and crossed terms for small  $\Omega$ :

$$\begin{aligned} L_2^{\text{inel}} &= \int_{-\infty}^{\infty} d\nu \tilde{L}_2^{\text{inel}}(\nu) = \frac{7}{16} \left(\frac{\Omega}{\gamma}\right)^4, \\ C_2^{\text{inel}} &= \int_{-\infty}^{\infty} d\nu \tilde{C}_2^{\text{inel}}(\nu) = \frac{3}{8} \left(\frac{\Omega}{\gamma}\right)^4. \end{aligned} \tag{27}$$

Combining Eq. (27) with the small- $s$  expression for the elastic ladder and crossed terms  $L_2^{\text{el}} = C_2^{\text{el}} = s$ , and rewriting Eq. (27) in terms of  $s$ , we recover the expected linear decrease

$$\alpha = 1 + \frac{s + 3s^2/2}{s + 7s^2/4} \approx 2 - \frac{s}{4}. \tag{28}$$

As the Rabi frequency  $\Omega$  increases further on (see Fig. 3b, 3c, 3d), qualitative differences emerge (on Fig. 3c, 3d) in the behavior of the ladder and crossed terms. First, the spectra split into several distinct peaks. Second, the crossed term becomes negative for a range of frequencies beyond the central peak. This is a manifestation of destructive self-interference of inelastically scattered photons. Note that a similar effect of anti-enhancement was reported [21] for linear double scattering from atoms with Zeeman shifted hyperfine ground levels. New spectral features are robust and become well-separated in the asymptotic limit of intense driving [for an example at  $\Omega = 100\gamma$ , see Fig. 3d]. In order to quantify the asymptotic CBS spectra, we will address the approximate analytic expression for it, derived in the leading order  $\sim(\gamma/\Omega)^2$ .

In this case, explicit expressions for CBS spectra can be represented by using a function of two real variables  $x_1$  and  $x_2$ :

$$\mathfrak{L}(x_1, x_2) = \frac{1}{\pi} \frac{x_1}{x_1^2 + x_2^2}. \tag{29}$$

Let us mention the properties of  $\mathfrak{L}(x_1, x_2)$  that are important to us: (i) if  $x_1 = \text{Const}$ , then function (29) represents a Lorentzian with width  $x_1$  and resonance at  $x_2 = 0$ ; (ii) if  $x_2 = \text{Const}$ , then (29) describes a resonance of a dispersive type at  $x_1 = 0$ .

With the help of the function (29), the ladder and crossed spectra are given by

$$\begin{aligned} \tilde{L}_2^{\text{inel}}(\nu) &\approx \left(\frac{\gamma}{\Omega}\right)^2 \left( \frac{1}{2} \mathfrak{L}(\gamma, \nu) + \frac{1}{4} \mathfrak{L}(3\gamma, \nu) + \right. \\ &+ \frac{1}{72} [\mathfrak{L}(3\gamma, \nu - 2\Omega) + \mathfrak{L}(3\gamma, \nu + 2\Omega)] + \\ &+ \frac{1}{9} [\mathfrak{L}(3\gamma/2, \nu - \Omega) + \mathfrak{L}(3\gamma/2, \nu + \Omega)] + \\ &+ \frac{5}{18} [\mathfrak{L}(5\gamma/2, \nu - \Omega) + \mathfrak{L}(5\gamma/2, \nu + \Omega)] + \\ &\left. + \frac{14}{9} [\mathfrak{L}(3\gamma/2, \nu - \Omega/2) + \mathfrak{L}(3\gamma/2, \nu + \Omega/2)] \right), \\ \tilde{C}_2^{\text{inel}}(\nu) &\approx \left(\frac{\gamma}{\Omega}\right)^2 \left( \frac{1}{2} \mathfrak{L}(2\gamma, \nu) + \frac{1}{4} \mathfrak{L}(3\gamma, \nu) - \right. \\ &- \frac{1}{6} [\mathfrak{L}(5\gamma/2, \nu - \Omega) + \mathfrak{L}(5\gamma/2, \nu + \Omega)] + \\ &+ \frac{1}{72} [\mathfrak{L}(3\gamma, \nu - 2\Omega) + \mathfrak{L}(3\gamma, \nu + 2\Omega)] \left. \right) + \\ &+ \left(\frac{\gamma}{\Omega}\right)^3 \frac{208}{45} [\mathfrak{L}(\nu + \Omega/2, 3\gamma/2) - \mathfrak{L}(\nu - \Omega/2, 3\gamma/2)], \end{aligned} \tag{30}$$

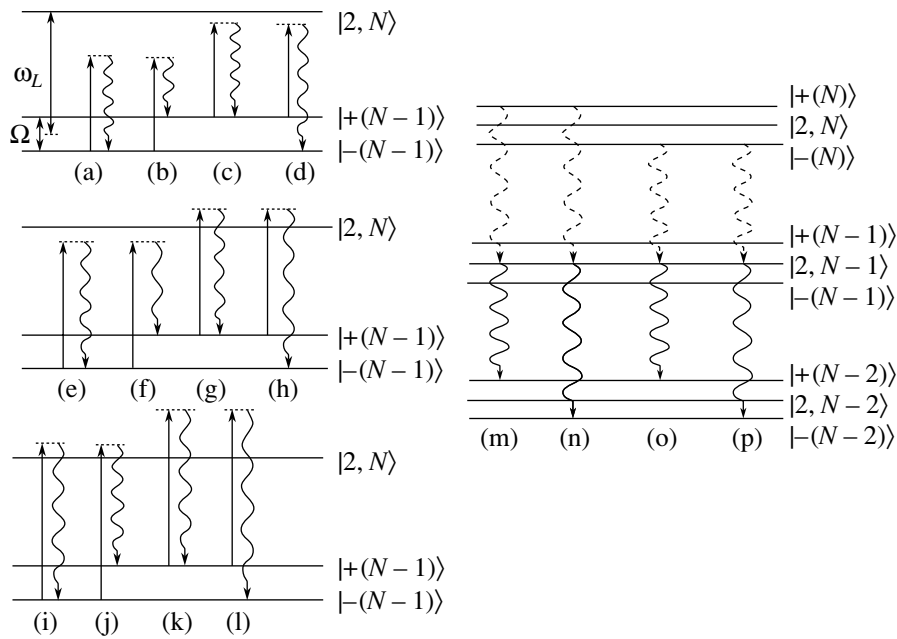


**Fig. 4.** Scattering processes (a–l) and radiative transitions (m–p), depicted by solid wavy arrows, contributing to CBS spectra in the regime of intense driving. Horizontal lines indicate dressed states. In processes (a–l), a photon with either of the frequencies emitted by one atom ( $\omega_L - \Omega$  (a–d);  $\omega_L$  (e–h);  $\omega_L + \Omega$  (i–l)) undergoes the Rayleigh or Raman scattering on the dressed states  $|\pm(N-1)\rangle$ . Diagrams (m–n) show radiative cascade in which CBS resonances at  $\omega_L \pm \Omega/2$  appear. Level  $|2, N\rangle$  can be populated as a result of a multiphoton scattering process with the participation of one doubly scattered photon (depicted by dashed wavy arrows).

where the two terms of order  $(\gamma/\Omega)^3$  are retained because they define dispersive resonances of  $\tilde{C}_2^{\text{inel}}$  ( $\nu$ ) at  $\nu = \pm\Omega/2$ . As seen from Eqs. (30) and (31) as well as from Fig. 3d, both the ladder and crossed terms have 7 resonances. All resonances of the ladder term are Lorentzians with positive weights. Two resonances of the crossed term at  $\nu = \pm\Omega/2$  have dispersive line shape. Furthermore, among the rest five resonances which all are of the Lorentzian type, two at  $\nu = \pm\Omega$  have negative weights. Thus, not all inelastic photons interfere with themselves constructively, yet the overall effect of all inelastic processes on interference is positive. Note also that in the frequency domains where interference is positive, it is also perfect, as can be concluded from the equality between the respective weights in the ladder and crossed contributions.

By performing the elementary integrations of Eqs. (30) and (31) we arrive at the inelastic ladder and crossed terms

$$L_2^{\text{inel}} \approx \frac{14}{3} \left(\frac{\gamma}{\Omega}\right)^2, \quad C_2^{\text{inel}} \approx \frac{4}{9} \left(\frac{\gamma}{\Omega}\right)^2, \quad (32)$$

which are consistent with Eqs. (23), (24) and, hence, with  $\alpha = \alpha_\infty = 23/21$ .

Let us now address the interpretation of the CBS spectrum in the limit of intense driving.

### C. Interpretation

One can understand the structure of the CBS spectrum from the analysis of CBS as a specific realization of the pump-probe experiment. In the usual setting of such an experiment [22], an atomic transition is simultaneously subjected to two monochromatic fields: a variable-intensity, fixed-frequency driving, or pump, field, and a weak probe field with tunable frequency. For different frequencies of the probe field it can be absorbed or amplified depending on the intensity of the pump field. This occurs because the pump field leads to the energy levels' shifts and broadenings, while the weak field transmission spectrum probes these new resonances; hence the name of this technique.

In our case of CBS with two atoms, an intense pump acts in the  $|1\rangle \leftrightarrow |4\rangle$  transitions of both atoms, causing an AC Stark shift of the energy levels. In this case it is instructive to treat the laser mode as a quantum system strongly coupled to the laser-driven atomic transition [23]. The eigenstates of the laser-atom interaction Hamiltonian for  $\delta = 0$  are the dressed states

$$|\pm(N)\rangle_\alpha = \frac{1}{\sqrt{2}}(|1, N+1\rangle_\alpha \pm e^{ikr_\alpha}|4, N\rangle_\alpha), \quad (33)$$

where  $N$  and  $N+1$  refer to the number of photons in the laser mode, and  $\alpha$  numbers the atoms. Spontaneous transitions from the dressed states manifold  $\{|\pm(N)\rangle_\alpha\}$  to  $\{|\pm(N-1)\rangle_\alpha\}$  lead to emission of the fluorescence spectrum with frequencies  $\omega_L - \Omega$ ,  $\omega_L$ , and  $\omega_L + \Omega$  known as the Mollow triplet [24]. The Mollow triplet

emitted by one atom plays a role of the probe for another atom. Whether this probe field is absorbed or amplified and what the contribution of interference is can be observed in the CBS spectrum.

Figure 4 illustrates the processes that contribute to the CBS spectrum in  $h \parallel h$  channel. Left part Fig. 4a–4l shows possible one-photon elastic Rayleigh and inelastic Raman processes which photons of frequencies  $\omega_L - \Omega$  (a–d),  $\omega_L$  (e–h), and  $\omega_L + \Omega$  (i–l) undergo on the dressed states  $|\pm(N-1)\rangle$ . One observes that there are 4 processes in which CBS photons with frequency  $\omega_L$  are created; 6 processes giving rise to frequencies  $\omega_L \pm \Omega$ ; 2 processes giving rise to  $\omega_L \pm 2\Omega$ . The latter processes represent true self-interference of inelastic photons at  $\omega_L - 2\Omega$  and  $\omega_L + 2\Omega$  leading to perfect enhancement (see Eqs. (30) and (31)). Right part of Fig. 4m–4n shows radiative cascade in the dressed state basis leading to resonances in the CBS spectrum at  $\omega_L \pm \Omega/2$ . These lines appear as a result of spontaneous transition from the state  $|2, N-1\rangle$  (note that the atomic state  $|2\rangle$  is not affected by the laser field) to states  $|\pm(N-2)\rangle$ .

Thus, in all the processes except (b) and (l), several transitions participate in the creation of a CBS photon. Phases between the participating transitions can be opposite due to difference, e.g., in initial, intermediate, or final atomic states, leading to negative signs of the interferential contributions around  $\omega_L \pm \Omega$  and  $\omega_L \pm \Omega/2$ . All in all, in the ‘pump-probe’ terminology, we observe that the probe field is amplified at all frequencies. A fuller analysis of CBS as a pump-probe experiment will be given in a future work.

#### 4. CONCLUSION

Using the master equation approach we have analytically calculated a spectrum of CBS by two identical, motionless atoms for the case of exact resonance between the laser and atomic transition frequencies. In particular, we have analysed the previously established [15, 16] effect of constructive self-interference of inelastically scattered photons.

Looking at the expressions for spectra [see Eqs. (30) and (31)], and at  $\alpha_\infty = 23/21$  expressing the overall effect of all inelastic processes, we come to the following conclusion. Enhancement factor based on the total backscattered light intensity is a poor measure of phase coherence between the counterpropagating waves in the saturation regime, because it conceals information on the character of interference at a given frequency. At intense driving, one should rather use spectrally resolved measurements with a filter whose passband  $\Gamma_f$  satisfies  $\gamma \ll \Gamma_f \ll \Omega$ . Then, tuning the filter on individual peaks of the CBS spectra, one would observe either perfect enhancement (at  $\omega = \omega_L$ ;  $\omega_L \pm 2\Omega$ ), or antienhancement (at  $\omega = \omega_L \pm \Omega$ ), else no net interference at all (at  $\omega = \omega_L \pm \Omega/2$ ).

We interpreted resonances of the asymptotic CBS spectra from regarding it as a pump-probe experiment. Although we relegated the detailed explanation of the character of interference between different processes, in which probe photons are scattered on the dressed states, to a separate work, the following remark is in order. For the exact resonance, some of the processes interfere constructively while some destructively, with the net effect being constructive. But it is possible to vary populations of the dressed states and, consequently, the weights of different processes by changing the laser detuning. Nothing forbids the overall effect of inelastic photons to be destructive. In fact, we showed in the previous work [16] that for large detuning it is indeed so. We also established in the same paper that the ladder term of double scattering becomes negative in  $h \perp h$  channel in the saturation regime. This result can be interpreted as a mere absorption of the probe field.

#### ACKNOWLEDGMENTS

I would like to thank Andreas Buchlietner and Cord Müller for the fruitful collaboration and encouragement which made this work possible. Useful discussions with Dominique Delande, Benoît Grémaud, Sergei Kilin, Dmitry Kupriyanov, Christian Miniatura, Alexander Nizovtsev, Marlan Scully, Igor Sokolov, Carlos Viviescas, and Thomas Wellens are gratefully acknowledged. Last not least, it is a pleasure to thank members of the Research Group ‘Nonlinear Dynamics in Quantum Systems’ at the Max Planck Institute for the Physics of Complex Systems for the friendly and creative atmosphere during my visits there.

#### REFERENCES

1. G. Labeyrie, F. de Tomasi, J.-C. Bernard, C.A. Müller, C. Miniatura, and R. Kaiser, *Phys. Rev. Lett.* **82**, 5266 (1999).
2. P. Kulatunga, C. I. Sukenik, S. Balik, M. D. Havey, D.V. Kupriyanov, and I.M. Sokolov, *Phys. Rev. A* **68**, 033816 (2003).
3. E. Akkermans, G. Montambaux, J.-L. Pichard, and J. Zinn-Justin (Eds.) *Mesoscopic Quantum Physics* (Elsevier, Amsterdam, 1994).
4. D. V. Kupriyanov, I. M. Sokolov, C. I. Sukenik, and M. D. Havey, *Laser Phys. Lett.* **3**, 223 (2006).
5. C. A. Müller, T. Jonckheere, C. Miniatura, and D. Delande, *Phys. Rev. A* **64**, 053804 (2001).
6. C. A. Müller and C. Miniatura, *J. Phys. A* **35**, 10163 (2002).
7. D. V. Kupriyanov, I. M. Sokolov, P. Kulatunga, C. I. Sukenik, and M. D. Havey, *Phys. Rev. A* **67**, 013814 (2003).
8. G. Labeyrie, D. Delande, C. A. Müller, C. Miniatura, and R. Kaiser, *Europhys. Lett.* **61**, 327 (2003).
9. T. Chanelière, D. Wilkowski, Y. Bidet, R. Kaiser, and C. Miniatura, *Phys. Rev. E* **70**, 036602 (2004).
10. T. Wellens, B. Grémaud, D. Delande, and C. Miniatura, *Phys. Rev. A* **70**, 023817 (2004).



11. T. Wellens, B. Grémaud, D. Delande, and C. Miniatura, *Phys. Rev. E* **71**, 055603(R) (2005); *Phys. Rev. A* **73**, 013802 (2006).
12. A. A. Golubentsev, *Zh. Eksp. Teor. Fiz.* **86**, 47 (1984) [*Sov. Phys. JETP* **59**, 26 (1984)].
13. G. Labeyrie, C. A. Müller, D. S. Wiersma, Ch. Miniatura, and R. Kaiser, *J. Opt. B: Quantum Semiclassical Opt.* **2**, 672 (2000).
14. D. V. Kupriyanov, I. M. Sokolov, N. V. Larionov, P. Kulatunga, C. I. Sukenik, S. Balik, and M. D. Havey, *Phys. Rev. A* **69**, 013814 (2004).
15. V. Shatokhin, C. A. Müller, and A. Buchleitner, **94**, 043603 (2005).
16. V. Shatokhin, C. A. Müller, and A. Buchleitner, **73**, 063813 (2006).
17. B. Grémaud, T. Wellens, D. Delande, C. Miniatura, unpublished.
18. R. J. Glauber, "Optical Coherence and Photon Statistics" in *Quantum Optics and Electronics*, edited by C. DeWitt, A. Blandin, and C. Cohen-Tannoudji (Gordon and Breach, London, 1965).
19. M. O. Scully and M. S. Zubairy, *Quantum Optics*, (Cambridge University Press, Cambridge, 1997).
20. R. H. Lehberg, *Phys. Rev. A* **2**, 883 (1970).
21. D. V. Kupriyanov, I. M. Sokolov, and M. D. Havey *Opt. Commun.* **243**, 165 (2004).
22. B. R. Mollow, **5**, 2217 (1972); F. Y. Wu, S. Ezekiel, M. Ducloy, and B. R. Mollow, **38**, 1077 (1977).
23. C. Cohen-Tannoudji, J. Dupont-Roc, and G. Grynberg, *Atom-Photon Interactions* (John Wiley & Sons Inc, New York, 1992).
24. B. R. Mollow, *Phys. Rev.* **188**, 1969 (1969).